

# Perturbative QCD Evolution and Color Dipole Picture

Dieter Schildknecht

Fakultät für Physik, Universität Bielefeld

D-33501 Bielefeld, Germany

and

Max-Planck Institute für Physik (Werner-Heisenberg-Institut),

Föhringer Ring 6, D-80805, München, Germany

## Abstract

The proton structure function in the diffraction region of small Bjorken- $x$  and  $10\text{GeV}^2 \leq Q^2 \leq 100\text{GeV}^2$  behaves as  $F_2(x, Q^2) = F_2(W^2) = f_0 \cdot (W^2)^{C_2}$ , where  $x = Q^2/W^2$ . The exponent  $C_2$  of the  $\gamma^*p$  center-of-mass energy squared,  $W^2$ , is predicted from evolution of the flavor-singlet quark distribution,  $C_2 = 0.29$ , and the only free parameter, the normalization  $f_0 = 0.063$ , is fitted. The evolution of the gluon density multiplied by  $\alpha_s(Q^2)$  is identical to the evolution of the flavor-singlet quark density. This simple picture is at variance with the standard approach to evolution based on the coupled equations of flavor-singlet and gluon density.

At sufficiently low values of the Bjorken variable,  $x \cong Q^2/W^2 \leq 0.1$ , the structure function for deep inelastic electron-proton scattering (DIS) is in good approximation of perturbative QCD (pQCD) dominated by the gluon density, or gluon distribution function, of the proton.

The longitudinal structure function of the proton in this approximation of low  $x$  and reasonably large  $Q^2$  is given by [1]

$$F_L(x, Q^2) = \frac{\alpha_s(Q^2)}{3\pi} \sum_q^{n_f} Q_q^2 6I_g(x, Q^2) \quad (1)$$

with

$$I_g(x, Q^2) \equiv \int_x^1 \frac{dy}{y} \left(\frac{x}{y}\right)^2 \left(1 - \frac{x}{y}\right) G(y, Q^2), \quad (2)$$

where  $G(y, Q^2) \equiv yg(y, Q^2)$ , and  $g(y, Q^2)$  stands for the gluon density. The sum over the (active) quark charges squared is denoted by  $\sum_q^{n_f} Q_q^2$ . Independently of the specific form of the gluon distribution, for a wide range of such distributions, the integration in (2) yields a longitudinal structure function directly proportional to the gluon distribution, but at a rescaled value of  $x \rightarrow \xi_L x$ ,

$$F_L(\xi_L x, Q^2) = \frac{\alpha_s(Q^2)}{3\pi} \sum_q^{n_f} Q_q^2 G(x, Q^2). \quad (3)$$

The rescaling factor in (3) has the preferred value of  $\xi_L \cong 0.40$ . [1].

The structure function  $F_2(x, Q^2)$  for  $x \leq 0.1$  in the DIS scheme is proportional to the flavor-singlet quark distribution,  $\Sigma(x, Q^2)$ . For  $n_f = 4$  flavors of quarks, we have

$$F_2(x, Q^2) = \frac{1}{4} \sum_q^{n_f} Q_q^2 \cdot x \Sigma(x, Q^2) = \frac{5}{18} x \Sigma(x, Q^2). \quad (4)$$

The evolution of the flavor-singlet quark distribution, and accordingly of  $F_2(x, Q^2)$ , with increasing virtuality,  $Q^2$ , of the photon,  $\gamma^*$ , is in good approximation determined by the gluon distribution according to [2, 3]

$$\frac{\partial F_2(\xi_2 x, Q^2)}{\partial \ln Q^2} = \frac{\alpha_s(Q^2)}{3\pi} \sum_q Q_q^2 G(x, Q^2). \quad (5)$$

In this case of  $F_2(x, Q^2)$  in (5), the rescaling factor is given by  $\xi_2 \cong 0.50$ .

By writing

$$F_L(x, Q^2) = \frac{1}{2\rho + 1} F_2(x, Q^2), \quad (6)$$

we introduce the ratio of the structure functions  $F_2(x, Q^2)$  and  $F_L(x, Q^2)$ . As long as  $\rho$  is allowed to vary with the kinematic variables,  $\rho = \rho(x, Q^2)$ , relation (6) amounts to a definition of the ratio of the longitudinal to the transverse photoabsorption cross section,

$$\frac{\sigma_{\gamma_{LP}^*}(x, Q^2)}{\sigma_{\gamma_{TP}^*}(x, Q^2)} = \frac{1}{2\rho}. \quad (7)$$

By replacing the right-hand side in (5) by (3), upon employing the definition (6), we obtain an evolution equation that solely contains the structure function  $F_2(x, Q^2)$  or, equivalently, the flavor-singlet distribution (4),

$$(2\rho + 1) \frac{\partial}{\partial \ln Q^2} F_2\left(\frac{\xi_L}{\xi_2} x, Q^2\right) = F_2(x, Q^2). \quad (8)$$

Similarly, by replacing the left-hand side in (6) by the gluon distribution according to (3), and inserting the result into (5), we find an equation for the gluon distribution that reads

$$\frac{\partial}{\partial \ln Q^2} (2\rho + 1) \alpha_s(Q^2) G\left(\frac{\xi_2}{\xi_L} x, Q^2\right) = \alpha_s(Q^2) G(x, Q^2). \quad (9)$$

Note that, without loss of generality,  $\rho = \rho(x, Q^2)$  is allowed, both in (8) and (9).

In the CDP [4], at sufficiently large  $Q^2$ , the structure functions become functions of the  $\gamma^*p$  center-of-mass energy,  $W$  [5, 6]<sup>1</sup> i.e.

$$F_{2,L}(x, Q^2) = F_{2,L}(W^2 = \frac{Q^2}{x}). \quad (10)$$

The dependence on the single variable  $W^2$  for a wide range of photon virtualities,  $Q^2$ , is consistent with the experimental data. Compare fig. 1, where we show <sup>2</sup> the experimental data [7] for  $F_2(x, Q^2)$  as a function of  $1/W^2$  for  $10\text{GeV}^2 \leq Q^2 \leq 100\text{GeV}^2$ .

In terms of the  $W$  dependence from (10), the evolution equation (8) reads

$$(2\rho_W + 1) \frac{\partial}{\partial \ln W^2} F_2\left(\frac{\xi_L}{\xi_2} W^2\right) = F_2(W^2), \quad (11)$$

where the notation  $\rho = \rho_W$  indicates that a potential  $W$  dependence of the ratio  $\rho$  from (6) and (7) on the kinematical variables, now  $W^2$ , is allowed in (11).

More specifically, we now assume a power law for the  $W$ -dependence of  $F_2(W^2)$  in (10),

$$F_2(W^2) = f_2 \cdot \left(\frac{W^2}{1\text{GeV}^2}\right)^{C_2} = f_2 \cdot \left(\frac{Q^2}{1\text{GeV}^2}\right)^{C_2} x^{-C_2}, \quad (12)$$

where the normalization  $f_2$  and the exponent  $C_2$  are constants. With (12), the evolution equation (11) yields,

$$(2\rho_W + 1) C_2 \left(\frac{\xi_L}{\xi_2}\right)^{C_2} = 1. \quad (13)$$

The conclusion (13) from the evolution equation (11) clearly rests on the  $W$  dependence of  $F_2(x, Q^2) = F_2(W^2 = Q^2/x)$  from the CDP combined with the

---

<sup>1</sup>The  $W$ -dependence in (10) is a consequence of the  $W$ -dependence of the color-dipole-proton cross section of the CDP [5, 6].

<sup>2</sup>We thank Prabhdeep Kaur for providing the plot of the experimental data.

power-law ansatz (12). According to (13), a constant value of the exponent  $C_2$  implies a constant value of  $\rho_W = \rho = \text{const}$  from (6) and (7), and vice versa.

In the CDP, the parameter  $\rho$  is associated with the enhanced transverse size [8, 9] of  $q\bar{q}$  fluctuations originating from transversely polarized photons,  $\gamma_T^*$ , relative to the transverse size of  $q\bar{q}$  fluctuations from longitudinally polarized photons,  $\gamma_L^*$ . The known distributions of the quark (antiquark) transverse momentum in transversely versus longitudinally polarized  $q\bar{q}$  fluctuations, via the uncertainty principle, imply an enhanced transverse size of transversely polarized  $q\bar{q}$  fluctuations. The size enhancement of definite magnitude yields an enhancement of the transverse relative to the longitudinal photoabsorption cross section in (7) and (6) that is quantitatively fixed by [8, 9]

$$\rho = \frac{4}{3}. \quad (14)$$

We note in passing that the factor 2 in (7) is due to the fact that the intensity of  $q\bar{q}$  pairs from transversely polarized photons in DIS at large  $Q^2$  is twice as large as the one from longitudinally polarized photons. This is in distinction from the factor  $\rho$  which is a property of the  $(q\bar{q})p$  interaction cross section.

The CDP prediction (14), according to (6), implies

$$F_L(x, Q^2) = 0.27 \cdot F_2(x, Q^2). \quad (15)$$

The prediction (15) is in agreement with the HERA measurements of  $F_L(x, Q^2)$  for small  $x$  and large  $Q^2$ . Compare refs. [8] and [9].

Substituting the empirically verified prediction (14) of  $\rho = 4/3$  into (13) together with the rescaling factors  $\xi_L = 0.40$  and  $\xi_2 = 0.50$  from (3) and (5), we find that  $C_2$  is determined to be equal to

$$C_2 = \frac{1}{2\rho + 1} \left( \frac{\xi_2}{\xi_L} \right)^{C_2} = 0.29. \quad (16)$$

We note that the result of  $C_2 = 0.29$  is fairly insensitive against variation of the ratio of the rescaling factors  $\xi_2$  and  $\xi_L$ . The (ad hoc) variation of this ratio in the interval of  $1 \leq \xi_2/\xi_L \leq 1.5$  around the preferred value of  $\xi_2/\xi_L = 1.25$ , according to (16), yields  $0.27 \leq C_2 \leq 0.31^3$ . Higher energies than the ones that were available at HERA are needed for a precision determination of  $C_2$  within this interval.

---

<sup>3</sup>Note that (16) differs from the result in ref.[10] by taking into account the rescaling factor  $\xi_L = 0.4$  as well as  $\rho = 4/3$ .

Returning to the experimental data for  $F_2 = F_2(W^2 = Q^2/x)$ , in fig. 1, we show the theoretical result from (12) for

$$F_2(W^2) = f_2 \cdot \left(\frac{W^2}{1\text{GeV}^2}\right)^{C_2} \equiv 0.063 \left(\frac{W^2}{1\text{GeV}^2}\right)^{0.29}, \quad (17)$$

where  $C_2 = 0.29$  is the theoretical result from (16), while the normalization,  $f_2 = 0.063$ , was determined by an “eye-ball” fit to the experimental data in fig. 1.

With only a single fitted parameter,  $f_2 = 0.063$ , we obtained a representation of the experimental data for  $F_2(x, Q^2)$  over a wide range of  $10\text{GeV}^2 \leq Q^2 \leq 100\text{GeV}^2$ . A more complete analysis of the experimental data will be presented in a forthcoming paper [9] where, within the CDP by refining the previous analysis [5], the extension of the description of the experimental data for  $F_2(x, Q^2)$  to  $Q^2 = 0$  and  $Q^2 > 100\text{GeV}^2$  is treated in detail.

We turn our attention to the evolution of the gluon density in (9). For  $\rho = \text{const}$ , compare (14), we have from (9)

$$(2\rho + 1) \frac{\partial}{\partial \ln Q^2} \alpha_S(Q^2) G\left(\frac{\xi_2}{\xi_L} x, Q^2\right) = \alpha_S(Q^2) G(x, Q^2). \quad (18)$$

Comparison of (18) with (8), taking into account (4), reveals that the evolution of  $\alpha_S(Q^2) G(x, Q^2)$ , i.e. the evolution of the gluon density multiplied by  $\alpha_S(Q^2)$ , coincides with the evolution of the flavor-singlet quark density<sup>4</sup>.

In the language of quark and gluon distributions, the forward-Compton-scattering amplitude of the CDP in fig.2 corresponds to  $\gamma^*$  gluon  $\rightarrow q\bar{q}$  fusion as shown in fig. 3. According to fig. 3, the evolution of the flavor-singlet quark distribution induced by the interacting photon,  $\gamma^*$ , of virtuality  $Q^2$  directly measures the evolution of the gluon distribution thus suggesting identical evolutions of the singlet quark distribution and the gluon distribution multiplied by the strong coupling  $\alpha_S(Q^2)$ , as obtained in (18).

Combining (3) with (6), and taking into account the  $W$  dependence from (10), we can directly deduce the gluon distribution from the (fit to the) experimental data in fig. 1,

$$\alpha_S(Q^2) G(x, Q^2) = \frac{3\pi}{(2\rho + 1) \sum_q Q_q^2} F_2\left(\frac{1}{\xi_L} W^2 = \frac{Q^2}{\xi_L x}\right), \quad (19)$$

---

<sup>4</sup>This result is at variance with the usual procedure that supplements the evolution equation for the flavor-singlet quark distribution by a separate equation for the gluon distribution. See discussion below.

where (17) is to be inserted on the right-hand side <sup>5</sup> together with  $\rho = 4/3$  from (14) and  $\sum_q Q_q^2 = 10/9$  for four active flavors.

Before confronting the gluon distributions obtained from (19) with the results available in the literature [12, 13] we briefly summarize the widely used procedure usually employed when deducing a gluon-distribution function from the experimental data on the structure function  $F_2(x, Q^2)$ .

The evolution equation for the flavor-singlet quark distribution is supplemented by an equation for the gluon distribution, obtained [2] by replacing the quarks in fig. 3 by (electromagnetically neutral) gluons, disregarding the photon, and replacing the gluon  $\rightarrow$  quark splitting in fig.3 by gluon  $\rightarrow$  gluon splitting. The resulting well-known coupled DGLAP equations [2], in connection with the fits [13, 14, 15, 16] to the experimental data on  $F_2(x, Q^2)$ , are then solved numerically.

The DGLAP gluon-evolution equation has an approximate analytic solution, the well-know double-asymptotic solution (DAS) [17] that is understood [2, 4] as resummation of a gluon ladder subject to certain “ordering assumptions” on the gluon momenta, compare fig.4. The DAS corresponds [4] to introducing an  $x$ -dependent generalized dipole cross section into the CDP, thus resolving the lower blob in fig.2. The  $x$ -dependence of the DAS of the DGLAP approach is at variance with our requirement of a  $W$ -dependent color-dipole cross section. It is precisely this  $W$  dependence that (within the CDP) allows [5, 9] for a transition to the region of  $Q^2 \rightarrow 0$ , including photoproduction by real photons.

Based upon an analysis employing the DAS of the DGLAP equations, the exponent,  $\lambda$ , of the Bjorken- $x$  dependence of the gluon distribution,  $G(x, Q^2) \sim x^{-\lambda}$ , was predicted [18] as  $\lambda = 0.32 \pm 0.05$ . This result is consistent with our prediction of  $C_2 = 0.29$  from (16), (17) and (19).

Application of DGLAP evolution to the “hard Pomeron” part of a Regge fit [13] to the experimental data for  $F_2(x, Q^2)$ , led to  $G(x, Q^2) \sim x^{-\epsilon_0}$ , where  $\epsilon_0 = 0.427$  is the fit parameter characterizing the (necessary) hard Pomeron contribution to the structure function,  $F_2(x, Q^2) \sim x^{-\epsilon_0}$ . While this  $x$  de-

---

<sup>5</sup>Note that from (19) with (17) the gluon distribution function can be extracted for any pair of values of  $x$  and  $Q^2$  with  $W^2 = Q^2/x$  for given  $W^2$ . Even though the underlying relations (3) and (6) do not hold for  $Q^2 \leq 10\text{GeV}^2$ , the gluon distribution from (19) remains sensible. The relation of the structure function to the gluon distribution becomes modified for  $Q^2 \rightarrow 0$ , while the  $W$ -dependent gluon distribution remains the one extracted from (19), compare ref.[9]. We note that our gluon distribution (19) is manifestly positive in distinction to some result in the literature (compare e.g. ref.[11])

pendence is somewhat stronger, the  $Q^2$  dependence of the gluon distribution extracted [13] from the Regge fit is somewhat weaker than ours that coincides with the  $x$  dependence and is determined by  $\alpha_S(Q^2)G(x, Q^2) \sim (Q^2)^{C_2} = (Q^2)^{0.29}$ .

The most elaborate and technically demanding numerical extractions of valence-quark as well as sea-quark and gluon distributions were carried out by so-called global fits to the experimental data of the structure function  $F_2(x, Q^2)$  by several collaborations [14, 15, 16]. Comparing the results of the different collaborations collected in the Durham Data Base [12], one finds a significant spread of the values of the extracted gluon distributions as a function of  $x$  as well as  $Q^2$ .

Our results for the gluon distribution from (19) with (17) lie within the range of the distributions from the hard Pomeron [13] and from refs.[14, 15, 16] as given by the Durham Data Base [12]. More details will be presented in [9].

In summary:

- i) By combining pQCD in the approximation (3) and (5) with the  $W$ -dependence of  $F_2(x, Q^2) = F_2(W^2 = Q^2/x)$  from the CDP, we find that the evolution equation for the flavor-singlet quark distribution predicts the exponent  $C_2 = 0.29$ , where  $F_2(W^2) \sim (W^2)^{C_2}$ . Only one fitted parameter, the normalization of  $F_2(W^2)$ , is required to represent  $F_2(W^2)$  for  $x < 0.1$  in the wide range of  $10\text{GeV}^2 \leq Q^2 \leq 100\text{GeV}^2$ . Our results for  $F_2(x, Q^2) = F_2(W^2)$  within the CDP of pQCD can be smoothly extended to  $Q^2 \rightarrow 0$ .
- ii) The evolution of the gluon-distribution function multiplied by  $\alpha_S(Q^2)$  is identical to the flavor-singlet evolution. This result is at variance with the results from the usual extraction of the gluon distribution that relies on supplementing the DGLAP evolution of the flavor-singlet quark distribution by the gluon-evolution equation.
- iii) Our gluon distribution is directly related to (the fit to) the experimental data for  $F_2(W^2)$  by a known proportionality constant. Our extraction of the (manifestly positive) gluon distribution from the experimental data is transparent, as far as the underlying theoretical assumptions and the relation to the experimental data are concerned, and it is straight forward and simple.

- iv) The results for the gluon distribution from the analysis of the experimental data by different collaborations differ significantly from each other. Within this wide range, our gluon distribution is compatible with the published ones, even though both, our underlying assumptions and our procedure, differ appreciably from the ones in the literature.

## Acknowledgement

I am grateful to Prabhdeep Kaur for providing the plot of the experimental data for the structure function.

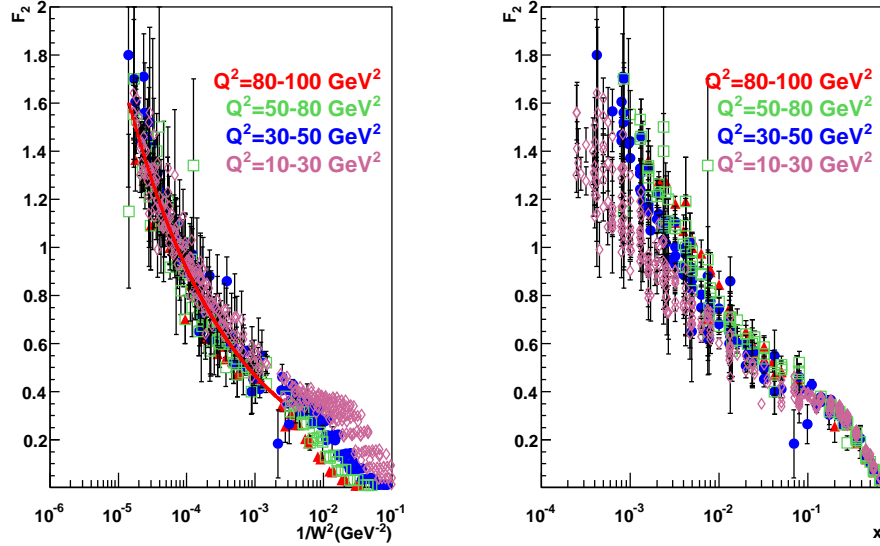


Figure 1: The experimental data on the proton structure function  $F_2(x, Q^2)$  as a function of  $1/W^2$ . The theoretical curve is based on (17). For comparison, we also show  $F_2(x, Q^2)$  as a function of  $x \cong Q^2/W^2$ .



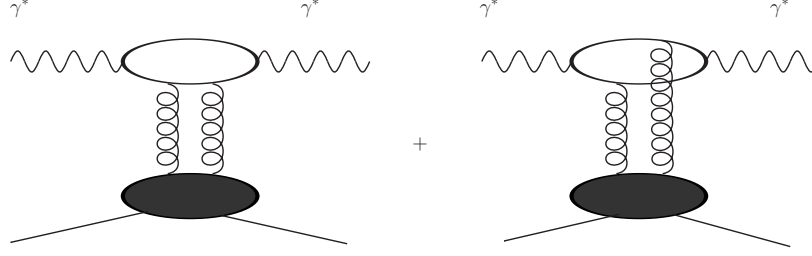


Figure 2: The forward Compton amplitude of the CDP

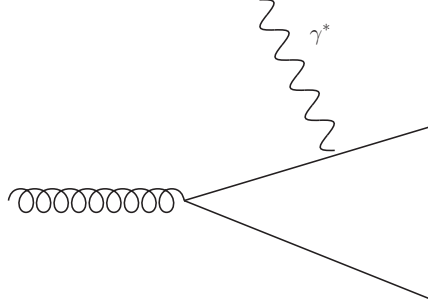


Figure 3: Photon-gluon  $\rightarrow q\bar{q}$  fusion, equivalent to the CDP from fig.1.

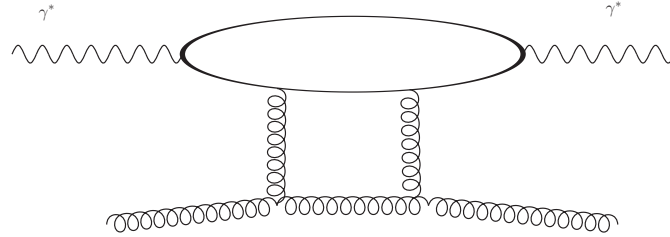


Figure 4: Higher order corrections to photon-gluon  $\rightarrow q\bar{q}$  fusion resolving the lower blob in fig.2. The lower part of the diagram must be extended to become a gluon ladder.

## References

- [1] A.D. Martin et al., Phys. Rev. D37 (1988) 1161;  
A.M. Cooper-Sarkar et al., Z. Phys. C39 (1988) 281.
- [2] L.N. Lipatov, Sov. J. Nucl. Phys. 20 (1975) 95;  
V.N. Gribov and L.N. Lipatov, Sov. J. Nucl. Phys. 15 (1972) 438;  
G. Altarelli and G. Parisi, Nucl. Phys. B126 (1977) 298;  
Yu. L. Dokshitzer, Sov. Phys. JETP 46 (1977) 641.
- [3] K. Prytz, Phys. Lett. B311 (1993) 286.
- [4] N.N. Nikolaev, B.G. Zakharov, Z. Phys. C 49 (1991) 607; Z. Phys. C64 (1994) 631.
- [5] D. Schildknecht, Contribution to Diffraction 2000, Centrarò, Italy, September 2-7, 2000, Nucl. Phys. B (Proc. Supplement) 99 (2001) 121;  
D. Schildknecht, B. Surrow, M. Tentyukov, Phys. Lett. B499 (2001) 116;  
G. Cvetic, D. Schildknecht, B. Surrow, M. Tentyukov, EPJC 20 (2001) 77;  
D. Schildknecht, B. Surrow, M. Tentyukov, Mod. Phys. Lett. A16 (2001) 1829.
- [6] C. Ewerz and O. Nachtmann, Annals of Physics 322 (2007) 1635; 322 (2007) 1670;  
C. Ewerz, A. v. Manteuffel, O. Nachtmann, arXiv:1101.0288 [hep-ph].
- [7] Durham Data Base, <http://durpdg.dur.ac.uk/HEPDATA/REAC>
- [8] M. Kuroda and D. Schildknecht, Phys. Lett. B670 (2008) 129.  
D. Schildknecht, Contribution to DIS2009, Madrid, April 25 to 30, 2009, arXiv0907.0545 [hep-ph]
- [9] M. Kuroda and D. Schildknecht, in preparation
- [10] M. Kuroda and D. Schildknecht, Phys. Lett. B618 (2005) 84.
- [11] A. Cooper-Sarkar, arXiv:0901.4001 [hep-ph].
- [12] Durham Data Base, <http://durpdg.dur.ac.uk/HEPDATA/PDF>.

- [13] A. Donnachie and P.V. Landshoff, Phys. Lett. B533 (2002) 277, hep-ph/0111427; Acta Physica Polonica B34 (2003) 2989, hep-ph/0305171.
- [14] M. Glück, E. Reya, A. Vogt, Z. Phys. C67 (1994) 433; Eur. Phys. J. C5 (1998) 461.
- [15] A.D. Martin, R.G. Roberts, W.J. Stirling and R.S. Thorne, Eur. Phys. J. C18 (2000) 117.
- [16] CTEQ collaboration: J. Pumplin et al., JHEP 0207 (2002) 012.
- [17] A. De Rujula et al., Phys. Rev. D10 (1974) 1649;  
R.D. Ball and S. Forte, Phys. Lett. B335 (1994) 77.
- [18] F. Caola and S. Forte, arXiv:0802.187802 [hep-ph], Phys. Rev. Letters 101 (2008) 022001.